Published in Environmental Science & Technology 39, issue 11, 4189-4197, 2005,
which should be used for any reference to this work

Quantification of Sequential Chlorinated Ethene Degradation by Use of a Reactive Transport Model Incorporating Isotope Fractionation

BORIS M. VAN BREUKELEN,*,† DANIEL HUNKELER,‡ FRANK VOLKERING§

Department of Hydrology and Geo-Environmental Sciences, Faculty of Earth and Life Sciences, Vrije Universiteit, De Boelelaan 1085, NL-1081 HV Amsterdam, The Netherlands
Centre for Hydrogeology, University of Neuchâtel, Rue Emile-Argand 11, CH-2007 Neuchâtel, Switzerland
Tauw bv, Post Office Box 133, NL-7400 AC Deventer, The Netherlands

Compound-specific isotope analysis (CSIA) enables quantification of biodegradation by use of the Rayleigh equation. The Rayleigh equation fails, however, to describe the sequential degradation of chlorinated aliphatic hydrocarbons (CAHs) involving various intermediates that are controlled by simultaneous degradation and production. This paper shows how isotope fractionation during sequential degradation can be simulated in a 1D reactive transport code (PHREEQC-2). ^{12}C and ^{13}C isotopes of each CAH were simulated as separate species, and the ratio of the rate constants of the heavy to light isotope equaled the kinetic isotope fractionation factor for each degradation step. The developed multistep isotope fractionation reactive transport model (IF-RTM) adequately simulated reductive dechlorination of tetrachloroethene (PCE) to ethene in a microcosm experiment. Transport scenarios were performed to evaluate the effect of sorption and of different degradation rate constant ratios among CAH species on the downgradient isotope evolution. The power of the model to quantify degradation is illustrated for situations where mixed sources degrade and for situations where daughter products are removed by oxidative processes. Finally, the model was used to interpret the occurrence of reductive dechlorination at a field site. The developed methodology can easily be incorporated in 3D solute transport models to enable quantification of sequential CAH degradation in the field by CSIA.

Introduction

The reductive dechlorination of chlorinated aliphatic hydrocarbons (CAHs) such as tetrachloroethene (PCE), trichloroethene (TCE), tetrachloromethane, and trichloroethane is characterized by temporary accumulation of lower chlorinated daughter products (*1*). Some of these daughter products such as dichloroethene (DCE) or vinyl chloride (VC) can be degraded by reductive dechlorination as well as by aerobic and anaerobic oxidation (*2*). The presence of daughter products can make interpretation of biodegradation in the field rather straightforward. However, if the daughter products are removed by oxidative processes, the demonstration of complete transformation to nontoxic products becomes difficult. Furthermore, the interpretation of concentration data can be complicated by the presence of lower chlorinated hydrocarbons as primary compounds at the source or by multiple compounds leading to the formation of the same daughter products (*3*). In these situations additional information is required to identify transformation processes.

Compound-specific stable carbon isotope analysis (CSIA) of chlorinated aliphatic hydrocarbons (CAHs) has been shown to be a valuable method to gain additional insight into CAH degradation in the field (*4*−*6*). During anaerobic microbial reductive dechlorination of chlorinated ethenes, the bonds containing light (^{12}C) versus heavy isotope (^{13}C) are cleaved slightly faster, resulting in isotopic enrichment of the residual contaminant in ^{13}C (*4*, *5*, *7*). Carbon isotope fractionation has also been observed during oxidation of *trans*-1,2-dichloroethene (tDCE) (*8*), 1,2-dichloroethane (*9*), dichlo-romethane (*10*), TCE, and VC but was close to zero for *cis*-1,2-dichloroethene (cDCE) (*11*). Other nondegradative processes such as dilution, sorption, volatilization, and dense nonaqueous phase liquid (DNAPL) dissolution involve only negligible isotope fractionation (*12*−*15*). Consequently, an increase in $\delta^{13}C$ signature reflects ongoing degradation, whereas a concentration decline without a change in $\delta^{13}C$ signature normally indicates nondegradative processes.

A simple closed-system Rayleigh model has been used to describe the relationship between the concentration and isotopic composition of an organic contaminant during biodegradation (*5*, *16*, *17*). However, where interpretation of stable isotope signatures of BTEX compounds during microbial breakdown is rather straightforward, for example, Mancini et al. (*16*), the sequential degradation of CAHs makes interpretation more complicated. The Rayleigh degradation model applies only to the parent compound of the sequential chain but not to its daughter products because they are affected by consumption and production simultaneously. Furthermore, the application of the Rayleigh model is inappropriate if several parent compounds such as PCE and TCE are simultaneously present as primary contaminants. Finally, the Rayleigh equation describes isotope fractionation in a closed system and cannot account for transport processes. The complex system of isotopic fractionation by sequential dechlorination and separation of the different compounds by transport processes may lead to counterintuitive phenomena. The quantitative interpretation of isotope data in these cases requires a reactive transport model that incorporates isotope fractionation as well as additional information about the variability of isotope fractionation.

This paper describes incorporation of isotope fractionation during sequential degradation into a reactive transport code and the contribution of this model to demonstrating and quantifying sequential degradation of chlorinated ethenes. Thereby this work addresses an important goal of field application of compound-specific isotope analysis, the reliable quantification of transformation processes by means of integrating stable isotope constraints into a coupled reaction-transport model (*5*, *6*). The model was verified for single-species degradation by comparison to the Rayleigh equation, and the model was confirmed for sequential degradation including sorption by simulation of a previously published microcosm experiment in which complete reduc-

* Corresponding author phone: +31-20-5987393; fax: +31-20-5989940; e-mail: boris.van.breukelen@falw.vu.nl.
† Vrije Universiteit.
‡ University of Neuchâtel.
§ Tauw.

tive dechlorination of PCE to ethene (ETH) occurred (*4*). Isotopic enrichment factors and Monod kinetic parameters were obtained by optimizing the model, by use of the nonlinear optimization program PEST (*18*). Transport scenarios adopting parameter values representative for generic conditions were simulated to illustrate the effect of sorption and of different degradation rate constant ratios among CAH species on the evolving isotope patterns downgradient. Furthermore, the strength of the model to quantify degradation is illustrated for situations where a mixed PCE/TCE source degrades and for situations where an intermediate product such as cDCE or VC accumulates or only slowly degrades either via direct oxidation or via reductive dechlorination followed by fast oxidation of the reaction product. Finally, the model is used to interpret occurrence of reductive dechlorination at a field site.

Experimental Procedures

Model Code. Simulations were performed with the PHREEQC-2 model code (*19*). The PHREEQC-2 model operates in batch mode or simulates advective transport, dispersion, diffusion, and sorption in one dimension (1D). While this paper discusses only 1D cases, the PHREEQC-2 module can also be implemented in the coupled MODFLOW/MT3DMS–PHREEQC-2 model PHT3D (*20*) to enable two- and three-dimensional (2D/3D) transport simulations.^{12}C and ^{13}C isotopes of a particular CAH were added in the model as separate species in absolute concentrations. Isotope signatures were calculated after the simulation. This approach has been applied recently in numerical reactive transport models of (1) a landfill leachate pollution plume (*21*) in order to simulate stable carbon isotope geochemical processes (degradation of dissolved organic carbon, carbonate mineral precipitation, degassing of CO_2 and CH_4, and methane oxidation including isotope fractionation) and (2) a riparian zone to simulate stable nitrogen isotope behavior during denitrification (*22*). This numerical approach allows simulation of complex field situations and is thereby a significant advance to analytical models on isotope fractionation during sequential reductive dechlorination (*23*, *24*).

Simulation of Isotope Fractionation during Degradation. A number of laboratory studies have shown that kinetic isotope fractionation during degradation of a compound remains constant (*25*). The degree of isotope fractionation is usually characterized by the kinetic isotope fractionation factor α_k, which relates the isotope ratio of the product $^{13}R(\Delta P)$, appearing in an infinitely short time (instantaneous product), to the isotope ratio of substrate $^{13}R(S)$:

$$^{13}R(\Delta P) = \frac{^{13}r_P}{^{12}r_P} = \frac{-^{13}r_S}{-^{12}r_S} = \alpha_k {}^{13}R(S) \quad (1)$$

where $^{13}r_P$ and $^{12}r_P$ are the production rates of ^{13}C and ^{12}C, respectively, of a particular daughter product and $^{13}r_S$ and $^{12}r_S$ are the degradation rates of ^{13}C and ^{12}C, respectively, of the corresponding parent compound. Note that the rate of formation of product corresponds to the negative of the rate of substrate consumption. It was shown mathematically that for reactions of any order (*26*) and also for Monod kinetics (*9*) the kinetic isotope fractionation factor α_k is indeed expected to be constant during degradation of the compound despite decreasing concentrations. The isotopic enrichment factor ϵ ($\epsilon < 0$) is equal to $1000(\alpha_k - 1)$. To incorporate isotope fractionation into PHREEQC-2, degradation rates for ^{13}C and ^{12}C are required. The degradation rate $^{12}r_S$ of the dominant ^{12}C isotope is defined to correspond to the overall degradation rate r_S of a particular CAH substrate (S) corrected for the proportion of ^{12}C to total carbon:

$$-^{12}r_S = {}^{12}r_P = -r_S\left(\frac{[^{12}S]}{[S]}\right) \quad (2)$$

The degradation rate $^{13}r_S$ of the ^{13}C isotope is obtained by combining eqs 1 and 2:

$$-^{13}r_S = {}^{13}r_P = -r_S\left(\frac{[^{13}S]}{[S]}\right)\alpha_k \quad (3)$$

The overall degradation rate can be any rate expression such as first-order or Monod kinetics. The numerical model reproduced the Rayleigh equation for zero-order, first-order, and Monod kinetics (results not shown).

Simulation of Sorption. Sorption results in negligible isotope fractionation (*14*, *15*). However, sorption may retard the spreading of CAHs substantially and to a different extent. For chlorinated ethenes, the degree of retardation by sorption is expected to decrease in the order PCE to ETH based on the decline in octanol–water partitioning coefficient (Table 1). Equilibrium sorption was simulated for the 1D transport scenarios. However, kinetic sorption was simulated to enable modeling of the microcosm experiment:

$$R_i = -k_m\left(c_i - \frac{s_i}{K_d}\right) \quad (4)$$

where R is the sorption rate, i is either ^{12}C or ^{13}C, k_m is the first-order mass-transfer coefficient, c_i is the aqueous concentration (molar), s_i is the sorbed concentration (molar), and K_d is the dimensionless solid–water partitioning coefficient.

The dimensionless solid–water partitioning coefficient, K_d, was calculated from:

$$K_d = K_{oc} f_{oc} \frac{\rho_b}{\epsilon} \quad (5)$$

where K_{oc} is the solid-phase organic carbon–water partitioning coefficient (liters per kilogram), f_{oc} is the fraction of organic carbon in the soil (dimensionless), ρ_b is the bulk density (kilograms per liter), and ϵ is the porosity (dimensionless). Values for K_{oc} were calculated from (*27*):

$$K_{oc} = 10^{0.81} K_{ow}{}^{0.56} \quad (6)$$

where K_{ow} is the octanol–water partitioning coefficient.

Model Parameters Used for the Simulation of Scenarios. Table 1 presents an overview of isotopic enrichment factors, degradation rate constants, octanol–water partitioning coefficients (K_{ow}), and dimensionless solid–water partitioning coefficients (K_d) for chlorinated ethenes and ethene (ETH) observed in the literature. Since in most cases ETH is found to be the end product of the reductive dechlorination process, further reduction of ETH to ethane is disregarded.

The adopted isotopic enrichment factors for all transport scenarios (Table 1) were the mean of the average values from the studies of Lollar et al. (*28*), Bloom et al. (*7*), and Slater et al. (*17*). Dimensionless solid–water partitioning coefficients (K_d; Table 1) were calculated following eqs 5 and 6 by use of octanol–water partitioning coefficients from Schwarzenbach et al. (*33*), a bulk density of 1.86 kg/L, a porosity of 0.3, and an organic carbon fraction of 0.5%, which is realistic for glaciofluvial silty sands (*35*). Sorption of ETH was neglected, since it sorbs least (Table 1).

Monod kinetics is the best approach to simulate CAH degradation according to Haston and McCarty (*36*), as the degradation rate approaches zero-order kinetics for con-

TABLE 1. Isotopic Enrichment Factors, Degradation Rate Constants, Octanol−Water Partitioning Coefficients, and Dimensionless Solid−Water Partitioning Coefficients for Chlorinated Ethenes and Ethene Found in Literature

study	PCE	TCE	cDCE	VC	ETH
Isotopic Enrichment Factor (ϵ)					
Lollar et al. (*28*)		−7.1			
Bloom et al.[a] (*7*)		−4.6 (−6.6, −2.5)	−15.1 (−14.1, −16.1)	−24.1 (−26.6, −21.5)	−3
Slater et al.[b] (*17*)	−5.2 ± 0.3	−13.8 ± 0.7	−20.4 ± 1.2	−22.4 ± 1.8	
adopted in simulations	−5.2	−8.5	−17.8	−23.2	
First-Order Degradation Rate Constants Reported in the Field (per year)					
Aronson and Howard (*29*): mean[c]	1.1	0.9		2.7	
Wiedemeier et al. (*1*): median[d]	1.1	1.1		2.9	
Suarez and Rifai (*30*): mean[e]	3.7	1.1	0.7	1.1	
Aziz et al. (*31*): median[f]	1.1	1.2	1.2	1.7	
Aziz et al. (*31*): mean[g]	1.4	1.5	3.5	3.6	
Aziz et al. (*31*): specific site[h]	2.0	1.0	0.7	0.4	
Clement et al. (*32*): specific site[i]	0.15	0.16	0.24	1.5	4.4
Octanol−Water Partitioning Coefficient (log K_{ow})					
Schwarzenbach et al. (*33*)	2.88	2.42	1.86	1.27	
EPA (*34*)	2.97	2.47	1.98	1.62	1.27
Dimensionless Solid−Water Partitioning Coefficient (K_d)					
adopted in simulations	8.2	4.5	2.2	1.0	

[a] Results from two separate enrichment culture bottles. [b] Average value with 95% confidence interval. [c] Mean of compilation of field and in situ microcosm studies. [d] Median of compilation of field-derived rate constants. [e] Mean of compilation of reductive dechlorination rate constants of field or in situ studies. [f] Median of compilation of field-derived rate constants. [g] Mean of compilation of field-derived rate constants. [h] Calibrated field rate constants at Cape Canaveral Air Station, Florida. [i] Calibrated field rate constants at the area 6 site on Dover Air Force Base, Delaware.

centrations above a few micromolar or above the low milligram per liter range and first-order kinetics at lower concentrations. While Monod kinetics was indeed required to simulate the microcosm experiment (see later), first-order kinetics were applied for the transport scenarios, which is a reasonable assumption for low concentration levels and is consistent with the practice of calculating first-order rate constants for field studies (Table 1). The tendency of chloroethene compounds to undergo reductive dechlorination appears to decrease with the number of chlorine substituents (*36*−*39*). Surprisingly, this tendency is not reflected in most compilations of first-order degradation rate constants reported in the field (Table 1). Rather, rate constants derived from the field show a slight tendency to increase in the order PCE to VC. Average or median values calculated from compilations may be somewhat biased, however, because (1) the number of studies is limited, (2) rate constants have usually not been determined for all four chlorinated ethenes at each site, and (3) one extremely fast rate or several rates of zero affect the calculated average considerably. At individual sites, rate constants are observed to increase as well as to decrease in the order PCE to VC (Table 1). The ratio of first-order degradation rate constants of parent compounds and daughter products largely determines the isotope evolution as will be shown later. Scenarios were therefore performed with decreasing as well as increasing first-order rate constants adopted from the two specific sites specified in Table 1.

Description of the Microcosm Experiment. The microcosm, prepared with aquifer material from a site in Toronto where complete dechlorination of PCE had been observed, is described in more detail in Hunkeler et al. (*4*). Briefly, the microcosm had a total volume of 250 mL and consisted of 6 g of wet aquifer material and 200 mL of site groundwater that had been purged with N_2 to remove chlorinated compounds, ethene, ethane, and methane. The microcosm was amended with methanol (1.6 mM or 50 ppm) and PCE (85 μM or 14 ppm; $\delta^{13}C = -27.3‰$).

Results and Discussion

Simulation of Sequential Degradation in a Laboratory Batch Experiment. The model was tested by simulating the microcosm experiment of Hunkeler et al. (*4*), where complete sequential reductive dechlorination of PCE to ETH was observed. Monod kinetics needed to be incorporated in the model to enable matching of the observed degradation kinetics (Figure 1). In addition, it was necessary to include lag phases since daughter products were not instantaneously observed: TCE was measured after 2 days, cDCE after 3 days, VC after 4 days, and ETH was produced only after 5 days. Finally, kinetic sorption of PCE was included because the initial PCE concentration of 85 μM dropped within 1 day to about 40 μM while TCE production had not occurred yet (Figure 1). A dimensionless solid−water partitioning coefficient (K_d) for PCE sorption of 1.125 and a mass transfer coefficient (k_m) of 7.5/day were chosen to reach sorption equilibrium within 1 day. Sorption of other CAHs having lower solid−water partitioning coefficients was discarded. The temporal discretization in the model was 0.2 day. Model calibration was performed with PEST (*18*) by optimizing the large number of model parameters simultaneously: isotopic enrichment factors, lag phases, maximum degradation rate constants (V_{max}), and half-saturation constants (K_s) for PCE, TCE, cDCE, and VC.

The model was able to match observations well (Figure 1). Only δ^{13}C-cDCE observations were consistently higher than predicted (Figure 1). Degradation rates for PCE (V_{max} = 31.7 μM/day, K_s = 2.7 μM) and TCE (V_{max} = 31.8 μM/day, K_s = 2.9 μM) were similar and highest; VC degradation rate was lowest and because of its high K_s value showed pseudo-first-order behavior (V_{max} = 94 μM/day, K_s = 232 μM); while the cDCE degradation rate was only slightly higher than that of VC and followed pseudo-zero-order kinetics (V_{max} = 6.9 μM/day, K_s = 0.015 μM). Lower δ^{13}C signatures for daughter products with respect to parent compounds and an overall increase of δ^{13}C during degradation were features captured well by the model. The isotopic enrichment factors (ϵ) obtained via calibration were −2.9‰ for PCE, −9.1‰ for TCE, −13.7‰ for cDCE, and −14.7‰ for VC degradation. These follow the same general trend but are somewhat different than estimated by Hunkeler et al. (*4*), using the difference in δ^{13}C between the initially formed dechlorination product and the corresponding precursor: −2‰ for PCE, −4‰ for TCE, −12‰ for cDCE, and −26‰ for dechlorination

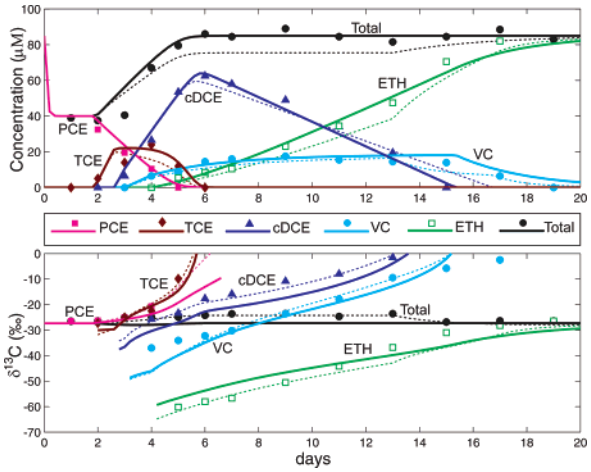

FIGURE 1. Simulation of sequential reductive dechlorination of chlorinated ethenes in a microcosm experiment. Lines are simulated values; symbols depict observations. Dashed lines are the results from the modified model.

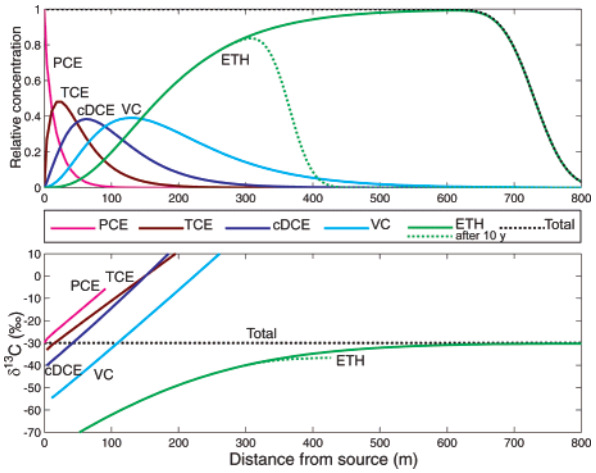

FIGURE 2. Transport simulation of 20 years of sequential reductive dechlorination of chlorinated ethenes, with decreasing rate constants. Dashed lines show results for ETH after 10 years.

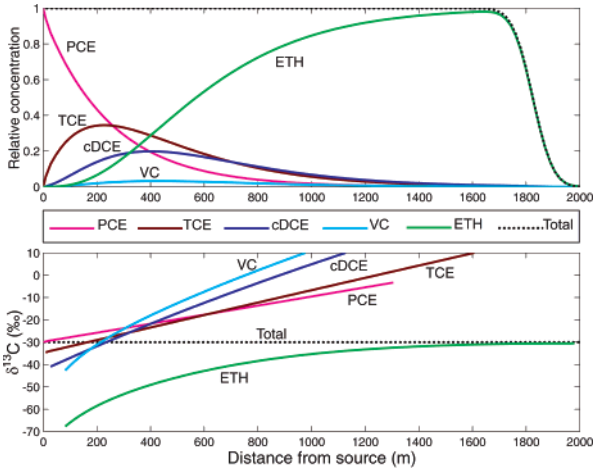

FIGURE 3. Transport simulation of 50 years of sequential reductive dechlorination of chlorinated ethenes, with increasing rate constants.

of VC to ETH. Adopting these latter isotopic enrichment factors did not improve the fit of cDCE, while δ^{13}C signatures for PCE and TCE were underestimated and δ^{13}C signatures of VC were overestimated.

Note that the isotope balance between days 3 and 13 is up to 3‰ too high, while the mass balance seems to match. The isotope imbalance for observations precludes a perfect model fit. The imbalance coincides with the accumulation of cDCE and is possibly due to the transient production of small amounts (<2.5 μM) of ^{13}C-depleted tDCE (*4*). Production of considerably more depleted tDCE than cDCE during enhanced bioremediation of TCE via lactate addition (*6*) suggests that kinetic isotopic fractionation for the TCE to tDCE step is much larger than for the TCE to cDCE step. Including the production and consumption of tDCE in a modified model allowed a better model fit, in particular for cDCE (Figure 1, dashed lines), and results in higher isotopic enrichment factors for cDCE (−17.8‰) and VC (−20‰) closer to values observed in the literature (Table 1). The modified model assumed an ϵ value for the TCE to tDCE step of −30‰ and adopted an ϵ value for the tDCE to VC step of −30.3‰ as observed by Hunkeler et al. (*23*). The following parameter values were adjusted in the modified model: an ϵ value for PCE of −5.2‰, resulting in a better fit for δ^{13}C of PCE; an ϵ value for TCE to cDCE of −6‰; a first-order degradation rate for TCE to tDCE and for tDCE to VC of 0.2/day and 0.3/day, respectively; and a V_{max} for cDCE and VC of 5.5 μM/day and 80 μM/day, respectively. Furthermore, the total degradation rate of VC was multiplied by a factor of 3 after day 13 to better describe the steep increase of the ETH concentration. The increase in the VC rate after day 13 is consistent with decreasing concentrations of cDCE, which can have an inhibitory effect on VC dechlorination (*40*). Degradation of tDCE was also assumed to occur only after day 13. The tDCE concentration did not exceed a concentration of 10 μM. A lower tDCE production rate resulting in lower tDCE concentrations together with a higher kinetic isotopic enrichment factor for the TCE to tDCE step resulted in similar outcomes. The successful simulation of this microcosm experiment shows that this model adequately predicts both concentrations and isotope signatures of CAHs and ETH during sequential degradation and sorption.

Simulation of Sequential Degradation during Transport. The purpose of these scenarios is to illustrate and discuss the effects of different degradation rate constant ratios among CAH species on the isotope evolution downgradient from a source zone. Two transport scenarios were evaluated by use of site-specific first-order rate constants in Table 1: one scenario with decreasing constants for the series PCE to VC and a second scenario with increasing but overall lower constants. A continuous PCE source concentration having a fixed isotope signature of −30‰ was simulated. A groundwater velocity of 0.1 m/day, a diffusion coefficient of 3×10^{-10} m^2/s, and a longitudinal dispersivity of 1 m were selected. To achieve (near) complete dechlorination downgradient, total transport times of 20 and 50 years were needed for the first and second scenarios, respectively.

Figure 2 shows the results for the transport scenario adopting decreasing degradation rate constants. Daughter products show lower isotope signatures than corresponding precursors while isotope signatures increase during degradation with distance from the source. Note that the cDCE isotope signature exceeds that of TCE only when TCE concentration becomes low. *cis*-Dichloroethene, having double the isotopic enrichment factor of TCE (Table 1), becomes enriched faster than TCE once its concentration and thereby its degradation rate becomes sufficiently high with respect to TCE. Since the model does not consider further ETH degradation, ETH accumulates and takes the original isotope signature of the source once dechlorination is complete. The concentration and isotope profiles resemble those described by Hunkeler et al. (*4*) at a field site where nearly complete dechlorination of PCE was observed (further discussed later).

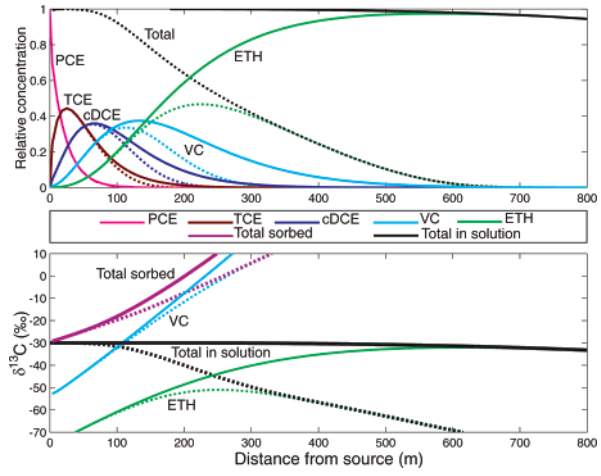

FIGURE 4. Transport simulation including sorption of sequential reductive dechlorination of chlorinated ethenes, with decreasing rate constants. Results for individual aqueous species and for the total of aqueous or sorbed species are shown after 20 years (dashed lines) and after 50 years (solid lines) of transport. Only isotope signatures for VC and ETH are presented for clarity.

The second scenario, using increasing degradation rate constants, leads to substantially different concentration and isotope patterns (Figure 3). Peak concentrations of CAHs become progressively lower in the order PCE to VC, whereas they were similar in the first scenario (Figure 2). In the second scenario, the intermediate product VC shows lowest concentration but degrades fastest. This simulation illustrates that faster degradation of daughter products together with increasing isotopic enrichment factors in the order PCE to VC cause isotope signatures of daughter products to exceed isotope signatures of parent compounds at some distance away from the source. Whereas isotope signatures are more depleted in the order PCE to VC near the source zone, the order becomes completely reversed further downgradient. Vinyl chloride becomes the most enriched CAH at about 300 m downgradient just behind the TCE peak. This scenario demonstrates that crossover of isotope ratios of daughter products to heavier values must be considered when data are interpreted. The presence of heavier products does not necessarily imply that an additional source is present. The two scenarios show that the isotope patterns of CAHs provide information on the relative rates of the intermediate steps within the overall dechlorination process.

Impact of Sorption on the Downgradient Isotope Evolution. Figure 4 presents the results of a third scenario, which is identical to the first scenario adopting decreasing rate constants (Figure 2) but includes sorption. Dimensionless solid−water partitioning coefficients (K_d) are listed in Table 1. The isotopic composition for each CAH in the aqueous and sorbed phase was identical, and the sorbed concentration was equal to the aqueous concentration multiplied by the K_d value (results not shown). Twenty and fifty years of transport were simulated. While PCE had reached a steady-state concentration and isotopic signature within 20 years, the other CAHs had not yet done so (Figure 4). After 50 years, ETH is only at steady state for the first 300−400 m away from the source, while other CAHs have reached steady-state profiles. The non-steady-state situation is characterized by lower isotope signatures and concentrations than at steady state. For example, at a hypothetical distance of 200 m downgradient, δ^{13}C values and relative concentrations for VC are −15.5‰ and 0.05 after 15 years and −7.6‰ and 0.3 after 40 years at steady-state conditions, respectively.

Sorption decreases the availability of CAHs in the water phase and thereby results in less degradation. Consequently, CAHs at the end of the degradation chain such as VC and ETH, which migrate faster than their precursors, have least developed concentration profiles compared to the steady-state situation. Sorption causes the total CAH concentration to decrease steadily downgradient for the non-steady-state part of the plume. However, sorption only slows down the development of concentration and isotope profiles and will result in roughly similar values as the nonsorbing case once steady state is reached. Slightly higher degradation rates were observed for the model without sorption (higher peaks of intermediates, steeper concentration decreases downgradient), and isotope lines were consequently also somewhat steeper.

Sorption affects the evolution of the isotope signature of the end product (in this case ETH) considerably. Whereas the ETH isotope signature initially increases away from the source zone as expected (Figure 2), at some point further away in the plume the effects of sorption lead to a subsequent decrease in δ^{13}C values (Figure 4). This point moves downgradient with time and with lower content of organic carbon in an aquifer until it disappears when organic carbon and thus sorption is absent (results of simulations not shown). Since the solid−water partitioning coefficient decreases in the order PCE to ETH, the depleted end product moves faster downgradient than its enriched precursors and its isotope signature is no longer affected by degradation of the parent compound (in this case VC). ETH at the front of the plume was produced from not-yet-enriched precursors when the source release started and is therefore very depleted. Sorption of enriched precursors results in an increase in δ^{13}C of total sorbed compounds away from the source (Figure 4). δ^{13}C of total aqueous compounds equals the source isotopic signature for the part of the plume that has reached steady state and decreases downgradient in the depleted front of the plume. Near-complete dechlorination is achieved after about 50 years at 600 m downgradient. In this steady-state part of the plume, δ^{13}C of total sorbed compounds remains enriched with respect to the source and is compensated by depleted ETH signatures at the not yet steady-state front part of the plume (further downgradient than shown in Figure 4).

Use of Isotope Analysis to Demonstrate Degradation of an Apparently Accumulating Intermediate Degradation Product. Reductive dechlorination of PCE or TCE is often observed to stop at cDCE or VC (*2*, *39*, *41*). Consequently, these intermediate products accumulate in the groundwater. Causes for accumulation are the absence of microorganisms able to transform cDCE or VC to ETH or conditions that are not sufficiently reducing (*39*). However, the accumulated cDCE or VC may be degraded by (1) direct oxidation of cDCE or VC (reaction pathway OX) or (2) reductive dechlorination of cDCE to VC followed by fast oxidation of the reaction product (reaction pathway RD) (*2*, *39*). These two reaction pathways are difficult to detect since the end products CO_2 and Cl^- are usually already present in groundwater.

Various scenarios were evaluated and are presented here in order to evaluate whether isotope analysis may demonstrate degradation of an apparently accumulating intermediate degradation product. The two proposed reaction pathways are likely characterized by different isotopic enrichment factors. For example, the isotopic enrichment factor for metabolic aerobic oxidation of VC ($\epsilon = -5.7$‰) is lower by a factor of 4 than for reductive dechlorination (*11*). Cometabolic VC oxidation results in even less isotope fractionation (*11*). The isotopic enrichment factor for (an)/aerobic oxidation of cDCE has not yet been determined but for cometabolic aerobic oxidation was close to 0 (*11*). However, the study tested only one cDCE-degrading strain and the experiment was carried out only until 50% cDCE degradation. The study on cometabolic cDCE degradation

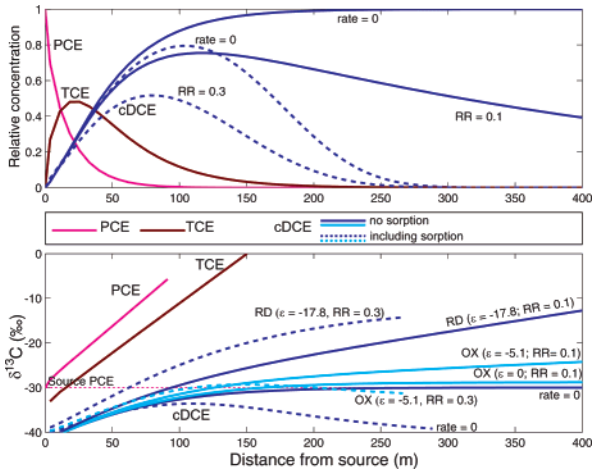

FIGURE 5. Demonstration of slow degradation of an accumulating intermediate daughter product (cDCE), omitting (solid lines) and including (dashed lines) sorption. Results are shown for both the OX and the RD degradation pathways and for different cDCE/TCE degradation rate constant ratios (RR).

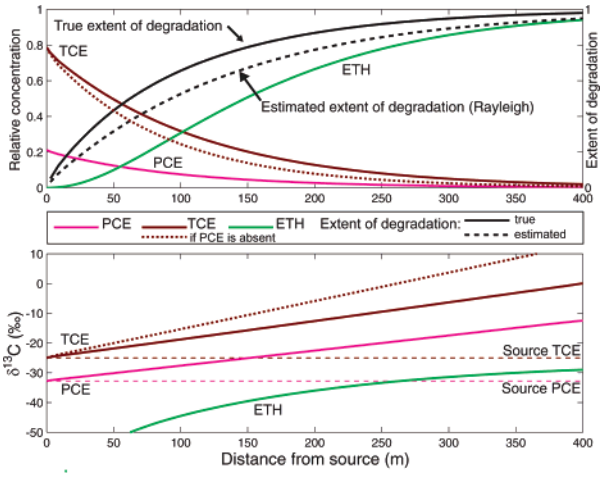

FIGURE 6. Isotope evolution downgradient from a mixed PCE/TCE source: consequences for quantification of TCE degradation by use of the Rayleigh model. Dashed lines for TCE show results when a PCE source is absent.

contrasts with a study on cometabolic tDCE degradation, which found isotopic enrichment factors of −3.5‰ and −6.7‰ (*8*). Although no studies are available to date, isotope fractionation for *metabolic* (an)aerobic oxidation of cDCE is probably substantially lower than for reductive dechlorination, similar to VC. Due to the uncertainty of the isotopic enrichment factor associated with oxidation of cDCE, two scenarios were modeled for reaction pathway OX, one with an enrichment factor of 0‰ and the other with an enrichment factor of −5.1‰, corresponding to the mean of the values from the tDCE study. For reaction pathway RD, a cDCE isotopic enrichment factor of −17.8‰ (mean for reductive dechlorination; Table 1) was chosen. Other model parameter values were identical to the earlier transport scenario, adopting decreasing degradation rate constants with or without sorption.

Absence of cDCE degradation results in a cDCE concentration and an isotopic signature downgradient identical to PCE in the source zone once all PCE and TCE have been degraded downgradient (Figure 5, rate = 0). Adopting a low cDCE degradation rate constant equal to 10% of the TCE degradation rate constant (relative rate RR = 0.1) results in cDCE isotopic signatures increasing downgradient and exceeding the isotopic signature of the PCE source zone at some point (Figure 5). This positive isotopic shift with respect to the source is a definite indicator for occurrence of biodegradation. The occurrence of reaction pathway RD will be easier to demonstrate than that of reaction OX because of the much larger shift toward more positive $\delta^{13}C$ values compared to the source. Interestingly, slow cDCE degradation without isotope fractionation will also result in cDCE signatures exceeding the source signature pointing out the occurrence of degradation. The isotopic shift was +1.2‰ for a rate constant ratio of 0.1 (Figure 5) and even +4.4‰ for a rate constant ratio of 0.3 at 400 m downgradient (result not shown). Removal by oxidation of lighter cDCE than average explains the occurrence of this shift even without isotope fractionation.

Sorption somewhat complicates the demonstration of degradation of an accumulating intermediate. As shown before in Figure 4 for ETH, the isotopic signature of the nondegrading end product will start to decrease at some point downgradient when sorption occurs instead of approaching the isotopic signature of the source. An analogous pattern of cDCE concentrations and $\delta^{13}C$ signatures, both decreasing downgradient from the cDCE peak, evolves during accumulation of cDCE (Figure 5, rate = 0, dashed line). One might interpret decreasing cDCE concentrations as degradation. However, nonincreasing cDCE isotope signatures indicate the lack of degradation. A positive isotopic shift of cDCE with respect to the source as a definite indicator for occurrence of biodegradation occurs only at a "threshold" cDCE degradation rate if sorption takes place. The cDCE/TCE rate constant ratio in this case must be at least 0.1 for reaction pathway RD (result not shown) or at least 0.3 for reaction pathway OX assuming an isotopic enrichment factor of −5.1‰ (Figure 5, RR = 0.3).

In principle, isotope analysis can demonstrate via a positive isotopic shift the occurrence of slow degradation of an accumulating intermediate when sorption is limited. The low kinetic isotopic fractionation involved with degradation via direct oxidation makes demonstration of this process more difficult than for reductive dechlorination followed by fast oxidation of the reaction product. Different combinations of enrichment factors and degradation rate constants may produce roughly similar isotope profiles. For example, the OX and RD pathways will produce roughly similar cDCE isotope profiles (but clearly different cDCE concentrations profiles) if the ratio of their first-order rate constants is comparable to the reciprocal of the ratio of their isotopic enrichment factors (results not shown). The relative effects of these two parameters can therefore be determined uniquely only by use of a model accounting for sorption and dilution and being constrained by isotope signatures as well as concentrations.

Mixed Sources: Interpretation of Signatures. Mixed source areas complicate interpretation of CAH degradation. We simulated the case of Dover Air Force Base, area 6 (*5*, *32*), to evaluate the effect of mixed source zones, containing both PCE and TCE, on the evolving isotope pattern. Well MW212 at this site was taken as a source (PCE, 541 μg/L and $\delta^{13}C$ = −32.8‰; TCE, 1590 μg/L and $\delta^{13}C$ = −25.0‰). First-order degradation rate constants (PCE, 0.15/year; TCE, 0.16/year; cDCE, 0.24/year; VC, 1.5/year) and dimensionless solid−water partitioning coefficients (K_d; PCE, 0.3; TCE, 0.2; cDCE, 0.1) were taken from a previous reactive transport model of sequential CAH degradation at this site (*32*). Isotopic enrichment factors were equal to the values adopted in the other scenarios. The total transport time of 40 years was equal to the age of the source areas. A groundwater flow rate of 14.4 m/year was adopted (*5*).

Results show that the high TCE isotope signature is diluted by simultaneous PCE degradation having a lower $\delta^{13}C$ (Figure

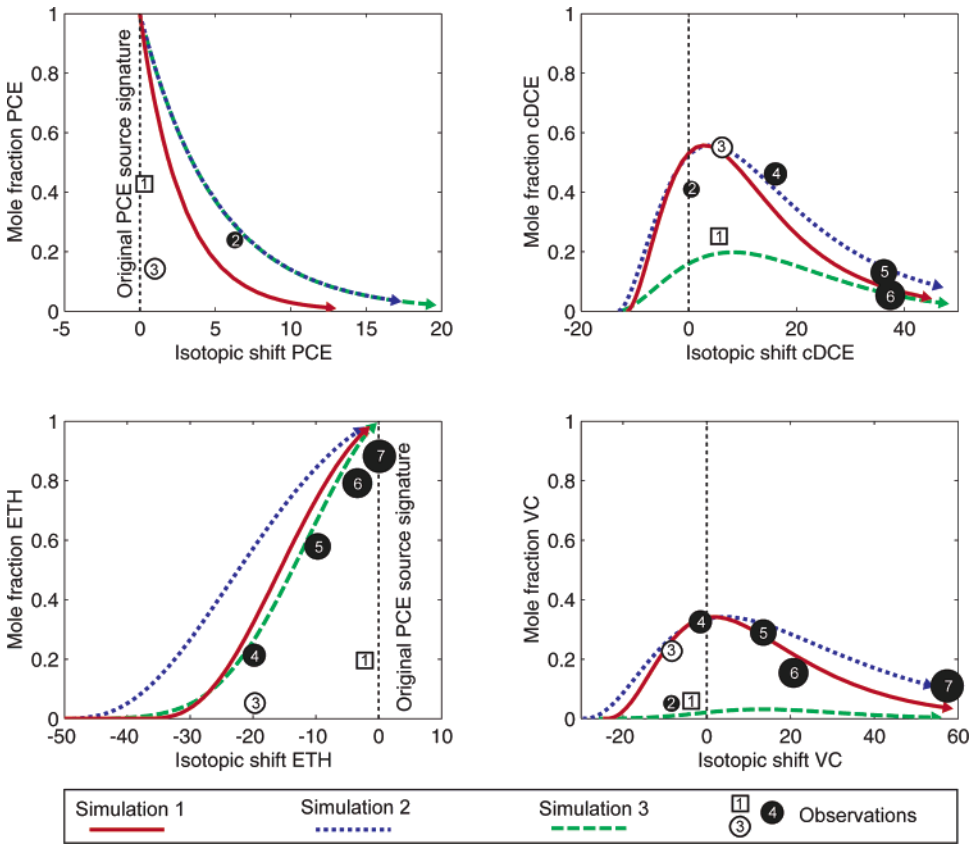

FIGURE 7. Simulation of reductive dechlorination at the Toronto field site. Lines are simulated values; symbols depict observations. Arrows indicate the direction of reaction progress. Open symbols are affected by mixing and/or dissolution of nonaqueous phase PCE. Observations correspond to the original codes for the monitoring wells at this site as follows, in order of increasing dechlorination extent: (1) CEL3, (2) CEL1, (3) CEL2, (4) CEL10, (5) ISRP 4-1, (6) ISRP 4-2, and (7) ISRP 5-1. Results for TCE are not shown for clarity.

6). Estimation of the extent of degradation by applying the Rayleigh equation will result in an underestimation of the true extent of degradation (considering additional TCE formation by PCE degradation) (Figure 6). The extent of underestimation is small for this case (a maximum difference in extent of degradation of 0.13 at 90 m downgradient) but will be more significant for higher PCE/TCE source ratios (here 0.27 mol/mol) and higher PCE/TCE degradation rate ratios (here 1:1.1). This case illustrates that degradation of a CAH can be truly quantified by use of the Rayleigh equation only when parent compounds are absent or are not being degraded, as indicated by a stable $\delta^{13}C$ value.

Application of the Model to a Field Site. We used the model to evaluate the rate constant ratios of the various degradation steps during reductive dechlorination of PCE at a field site in Toronto where concentrations and $\delta^{13}C$ of all CAHs and ETH were measured (*4*). The microcosm experiment simulated before was based on aquifer sediment from this site. The 1D model could not be directly applied because the observation wells were not placed along a flow path and the groundwater flow direction and velocity were poorly defined. Furthermore, the variable extent of dilution and/or artificial mixing induced by the long well screens resulted in a wide range of the total CAH + ETH concentration. However, relating the mole fraction to the isotopic shift with respect to the source PCE signature (e.g., $\delta^{13}C - \delta^{13}C_{sourcePCE}$) for each CAH and ETH allowed for a spatially and temporally independent comparison between the model and observations (Figure 7). This relationship is solely dependent on the kinetic isotopic enrichment factors and the rate constant ratios of the CAHs if first-order kinetics apply. Sorption affects this relationship only for non-steady-state conditions. Although absolute degradation rates cannot be quantified since spatial and temporal dimensions are not considered, the model allows evaluation of the relative rates of the various steps in the dechlorination network.

Figure 7 presents the results of three simulations performed in batch mode, applying first-order degradation without sorption, to illustrate the effects of different rate constant ratios and different sets of kinetic isotopic enrichment factors (ϵ). Simulation 1 used ϵ values from the microcosm experiment neglecting tDCE production (PCE, −2.9‰; TCE, −9.1‰; cDCE, −13.7‰; VC, −14.7‰), while the rate constant ratios (PCE:TCE:cDCE:VC 1:1.3:0.27:0.27) were adjusted manually to maximize the fit between simulated and measured data. Simulation 2 used the same relative rate contants and the average isotopic enrichment factors from the literature (Table 1) to evaluate how sensitive the simulation is to varying isotopic enrichment factors. Simulation 3 is similar to simulation 2 but used the rate constants increasing in the order PCE to VC (PCE:TCE:cDCE:VC 1:1.1:1.6:10) like the scenario shown in Figure 3. The observations are numbered with increasing extent of dechlorination. The $\delta^{13}C$ of PCE at well 3 and the $\delta^{13}C$ of ETH at well 1 were previously observed to deviate from the general trend toward more enriched $\delta^{13}C$ values with increasing dechlorination (*4*). Absence of an isotopic shift for PCE at well 3 and the highly enriched isotopic signature for ETH at well 1, although both are present at low mole fractions (Figure 7), indicate that (1) groundwater in which dechlorination had progressed to a large extent may have flown to areas where nonaqueous phase PCE is still dissolving and/or (2) waters from different layers in which dechlorination had progressed to a different extent may have been mixed during sampling. Wells 1 and 3 have indeed longer screened intervals (2.5 m) than the other wells (1.4 or 1.5 m).

Simulation 1 described the general trends as observed in the field reasonably (Figure 7). As in the microcosm experi-

ment, an isotopic enrichment factor of −5.2‰ adopted in simulations 2 and 3 matched the PCE observation in well 2 more closely than a value of −2.9‰ (Figure 7). Figure 7 illustrates the general pattern of the intermediate compounds cDCE and VC: mole fractions first increase and subsequently decrease while $\delta^{13}C$ continuously increases during degradation. Simulation 2, adopting the average literature ϵ values, described ETH observations poorly. Simulation 3, adopting increasing rate constants, resulted in a better fit for ETH but is unrealistic since predicted mole fractions for cDCE and VC were too low. Note that the end product ETH reached the original source signature already at a mole fraction of 0.88 in well 7. Apparently, mixing of waters in which dechlorination had progressed to a different extent may also have occurred to a lesser degree for the other samples, explaining the discrepancy between the model and observations. Despite the complexity of this field site, the model was able to describe observations reasonably. Scenarios 1 and 2 indicate that the first-order degradation rate constants for the latter two degradation steps (cDCE and VC) were about a factor of 4−5 lower than for the first two degradation steps (PCE and TCE) during dechlorination at this site.

Implications. The presented model greatly enhances the value of compound-specific isotope analysis for demonstrating occurrence of CAH degradation in the field. The model enables quantification of sequential degradation via calibration on both concentrations and isotope signatures. Comparison to the Rayleigh equation verified the model for single-species degradation, while simulation of the microcosm experiment confirmed the model for sequential degradation including sorption. The model can cope with sources of mixed composition and also accounts for sorption. The model can easily be extended with competitive TCE degradation pathways (from TCE to VC via tDCE or 1,1-DCE) and chlorine isotope fractionation (*42*, *43*) of CAHs following the same approach. The model could also be broadened to quantify the degradation of pollutants in other sequential degradation pathways (e.g., trichloroethane to ethane and tetrachloromethane to methane) or in parallel coupled degradation pathways (e.g., mixture of chlorinated ethenes and ethanes). The present PHREEQC-2 model can be implemented in the coupled MT3DMS−PHREEQC-2 model PHT3D (*20*) to enable 2D/3D simulations and thereby account for dilution, mixing of multiple plumes, and isotope fractionation as a result of oxidation at fringes of plumes. The model approach could in principle also be integrated in multiple solute transport models such as RT3D (*44*). Although calibration of a site-specific model is still a challenge remaining, the model approach is indispensable to evaluate isotope ratios in complex field settings and thereby to guide monitoring and remediation efforts.

Acknowledgments

We thank two anonymous reviewers for their thorough reviews and suggestions, which led to some major improvements. D.H. thanks the Swiss National Science Foundation for financial support.

Supporting Information Available

PHREEQC input file for the transport model on isotope fractionation during sequential PCE degradation (results shown in Figure 2). This material is available free of charge via the Internet at http://pubs.acs.org.

Literature Cited

(1) Wiedemeier, T. H.; Rifai, H. S.; Newell, C. J.; Wilson, J. T. *Natural attenuation of fuels and chlorinated solvents in the subsurface*; John Wiley & Sons: New York, 1999.

(2) Bradley, P. M. Microbial degradation of chloroethenes in groundwater systems. *Hydrogeol. J.* **2000**, *8*, 104−111.

(3) Hunkeler, D.; Aravena, R.; Cox, E. In *Remediation of Chlorinated and Recalcitrant Compounds-2002*; Gavaskar, A. R., Chen, A. S. C., Eds.; Battelle Press: Columbus, OH, and Monterey, CA, 2002.

(4) Hunkeler, D.; Aravena, R.; Butler, B. J. Monitoring microbial dechlorination of tetrachloroethene (PCE) in groundwater using compound-specific stable carbon isotope ratios: Microcosm and field studies. *Environ. Sci. Technol.* **1999**, *33*, 2733−2738.

(5) Lollar, B. S.; Slater, G. F.; Sleep, B.; Witt, M.; Klecka, G. M.; Harkness, M.; Spivack, J. Stable carbon isotope evidence for intrinsic bioremediation of tetrachloroethene and trichloroethene at area 6, Dover Air Force Base. *Environ. Sci. Technol.* **2001**, *35*, 261−269.

(6) Song, D. L.; Conrad, M. E.; Sorenson, K. S.; Alvarez-Cohen, L. Stable carbon isotope fractionation during enhanced in situ bioremediation of trichloroethene. *Environ. Sci. Technol.* **2002**, *36*, 2262−2268.

(7) Bloom, Y.; Aravena, R.; Hunkeler, D.; Edwards, E.; Frape, S. K. Carbon isotope fractionation during microbial dechlorination of trichloroethene, *cis*-1,2-dichloroethene and vinyl chloride: implication for assessment of natural attenuation. *Environ. Sci. Technol.* **2000**, *34*, 2768−2772.

(8) Brungard, K. L.; Munakata-Marr, J.; Johnson, C. A.; Mandernack, K. W. Stable carbon isotope fractionation of *trans*-1,2-dichloroethylene during co-metabolic degradation by methanotrophic bacteria. *Chem. Geol.* **2003**, *195*, 59−67.

(9) Hunkeler, D.; Aravena, R. Evidence of substantial carbon isotope fractionation between substrate, inorganic carbon, and biomass during aerobic mineralization of 1,2-dichloroethene by *Xanthobacter autotrophicus*. *Appl. Environ. Microbiol.* **2000**, *66*, 4870−4876.

(10) Heraty, L. J.; Fuller, M. E.; Huang, L.; Abrajano, T.; Sturchio, N. C. Isotope fractionation of carbon and chlorine by microbial degradation of dichloromethane. *Org. Geochem.* **1999**, *30*, 793−799.

(11) Chu, K.-H.; Mahendra, S.; Song, D. L.; Conrad, M. E.; Alvarez-Cohen, L. Stable carbon isotope fractionation during aerobic biodegradation of chlorinated ethenes. *Environ. Sci. Technol.* **2004**, *38*, 3126−3130.

(12) Huang, L.; Sturchio, N. C.; Abrajano, T.; Heraty, L. J.; Holt, B. D. Carbon and chlorine isotope fractionation of chlorinated aliphatic hydrocarbons by evaporation. *Org. Geochem.* **1999**, *30*, 777−785.

(13) Hunkeler, D.; Chollet, N.; Pittet, X.; Aravena, R.; Cherry, J. A.; Parker, B. L. Effect of source variability and transport processes on carbon isotope ratios of TCE and PCE in two sandy aquifers. *J. Contam. Hydrol.* **2004**, *74*, 265−282.

(14) Slater, G. F.; Ahad, J. M. E.; Lollar, B. S.; Allen-King, R.; Sleep, B. Carbon isotope effects resulting from equilibrium sorption of dissolved VOCs. *Anal. Chem.* **2000**, *72*, 5669−5672.

(15) Schüth, C.; Taubald, H.; Bolaño, N.; Maciejczyk, K. Carbon and hydrogen isotope effects during sorption of organic contaminants on carbonaceous materials. *J. Contam. Hydrol.* **2003**, *64*, 269−281.

(16) Mancini, S. A.; Lacrampe-Couloume, G.; Jonker, H.; Van Breukelen, B. M.; Groen, J.; Volkering, F.; Lollar, B. S. Hydrogen isotopic enrichment: An indicator of biodegradation at a petroleum hydrocarbon contaminated field site. *Environ. Sci. Technol.* **2002**, *36*, 2464−2470.

(17) Slater, G. F.; Lollar, B. S.; Sleep, B. E.; Edwards, E. A. Variability in carbon isotopic fractionation during biodegradation of chlorinated ethenes: Implications for field applications. *Environ. Sci. Technol.* **2001**, *35*, 901−907.

(18) Watermark Numerical Computing. http://www.sspa.com/pest.

(19) Parkhurst, D. L.; Appelo, C. A. J. *User's guide to PHREEQC (Version 2): a computer program for speciation, batch-reaction, one-dimensional transport, and inverse geochemical calculations*; U.S. Geological Survey: Denver, CO, 1999.

(20) Prommer, H.; Barry, D. A.; Zheng, C. MODFLOW/MT3DMS-based reactive multicomponent transport modeling. *Ground Water* **2003**, *41*, 247−257.

(21) Van Breukelen, B. M.; Griffioen, J.; Röling, W. F. M.; van Verseveld, H. W. Reactive transport modelling of biogeochemical processes and carbon isotope geochemistry inside a landfill leachate plume. *J. Contam. Hydrol.* **2004**, *70*, 249−269.

(22) Chen, D. J. Z.; MacQuarrie, K. T. B. Numerical simulation of organic carbon, nitrate, and nitrogen isotope behavior during denitrification in a riparian zone. *J. Hydrol.* **2004**, *293*, 235−254.

(23) Hunkeler, D.; Aravena, R.; Cox, E. Carbon isotopes as a tool to evaluate the origin and fate of vinyl chloride: Laboratory experiments and modeling of isotope evolution. *Environ. Sci. Technol.* **2002**, *36*, 3378−3384.

(24) Béranger, S. C.; Sleep, B. E.; Lollar, B. S.; Monteagudo, F. P. Transport, biodegradation and isotopic fractionation of chlorinated ethenes: modeling and parameter estimation methods. *Adv. Water Resour.* **2005**, *28*, 87−98.
(25) Schmidt, T. C.; Zwank, L.; Elsner, M.; Berg, M.; Meckenstock, R. U.; Haderlein, S. B. Compound-specific stable isotope analysis of organic contaminants in natural environments: a critical review of the state of the art, prospects, and future challenges. *Anal. Bioanal. Chem.* **2004**, *378*, 283−300.
(26) Bigeleisen, J.; Wolfsberg, M. Theoretical and experimental aspects of isotope effects in chemical kinetics. *Adv. Chem. Phys.* **1958**, *1*, 15−76.
(27) Valsaraj, K. T.; Kommalapati, R. R.; Robertson, E. D.; Constant, W. D. Partition constants and adsorption desorption hysteresis for volatile organic compounds on soil from a Louisiana superfund site. *Environ. Monit. Assess.* **1999**, *58*, 225−241.
(28) Lollar, B. S.; Slater, G. F.; Ahad, J.; Sleep, B.; Spivack, J.; Brennan, M.; MacKenzie, P. Contrasting carbon isotope fractionation during biodegradation of trichloroethylene and toluene: Implications for intrinsic bioremediation. *Org. Geochem.* **1999**, *30*, 813−820.
(29) Aronson, D.; Howard, P. H. *Anaerobic Biodegradation of Organic Chemicals in Groundwater: a Summary of Field and Laboratory Studies*; American Petroleum Institute: Washington, DC, 1997.
(30) Suarez, M. P.; Rifai, H. S. Biodegradation rates for fuel hydrocarbons and chlorinated solvents in groundwater. *Bioremed. J.* **1999**, *3*, 337−362.
(31) Aziz, C. E.; Smith, A. P.; Newell, C. J.; Gonzales, J. R. *BIOCHLOR Chlorinated solvent plume database report*; Air Force Center for Environmental Excellence (AFCEE): San Antonio, TX, 2000.
(32) Clement, T. P.; Johnson, C. D.; Sun, Y. W.; Klecka, G. M.; Bartlett, C. Natural attenuation of chlorinated ethene compounds: model development and field-scale application at the Dover site. *J. Contam. Hydrol.* **2000**, *42*, 113−140.
(33) Schwarzenbach, R. P.; Gschwend, P. M.; Imboden, D. M. *Environmental Organic Chemistry*; Wiley-interscience: New York, 2003.
(34) EPA. *EPI (Estimation Program Interface) Suite*; U.S. Environmental Protection Agency: Washington, DC, 2000.
(35) EPA. *Technical protocol for evaluating natural attenuation of chlorinated solvents in groundwater*; U.S. Environmental Protection Agency: Washington, DC, 1998.
(36) Haston, Z. C.; McCarty, P. L. Chlorinated ethene half-velocity coefficients (K_s) for reductive dehalogenation. *Environ. Sci. Technol.* **1999**, *33*, 223−226.
(37) Vogel, T. M.; Criddle, C. S.; McCarty, P. L. Transformations of halogenated aliphatic compounds. *Environ. Sci. Technol.* **1987**, *21*, 722−736.
(38) Magnuson, J. K.; Stern, R. V.; Gossett, J. M.; Zinder, S. H.; Burris, D. R. Reductive dechlorination of tetrachloroethene to ethene by two-component enzyme pathway. *Appl. Environ. Microbiol.* **1998**, *64*, 1270−1275.
(39) Bradley, P. M. History and ecology of chloroethene biodegradation: a review. *Bioremed. J.* **2003**, *7*, 81−109.
(40) Cupples, A. M.; Spormann, A. M.; McCarty, P. L. Comparative evaluation of chloroethene dechlorination to ethene by *Dehalococcoides*-like microorganisms. *Environ. Sci. Technol.* **2004**, *38*, 4768−4774.
(41) McCarty, P. L. Microbiology − Breathing with chlorinated solvents. *Science* **1997**, *276*, 1521−1522.
(42) Numata, M.; Nakamura, N.; Koshikawa, H.; Terashima, Y. Chlorine isotope fractionation during reductive dechlorination of chlorinated ethenes by anaerobic bacteria. *Environ. Sci. Technol.* **2002**, *36*, 4389−4394.
(43) Sturchio, N. C.; Clausen, J. L.; Heraty, L. J.; Huang, L.; Holt, B. D.; Abrajano, T. A. Chlorine isotope investigation of natural attenuation of trichloroethene in an aerobic aquifer. *Environ. Sci. Technol.* **1998**, *32*, 3037−3042.
(44) Clement, T. P.; Sun, Y.; Hooker, B. S.; Petersen, J. N. Modeling multispecies reactive transport in ground water. *Ground Water Monit. Remediat.* **1998**, *18*, 79−92.